Assessment of Using UAV Imagery over Featureless Surfaces for Topographic Applications

Ahmed Taha
Lecturer, Department of Civil Engineering, Benha Faculty of Engineering, Benha University, Egypt, ahmed.soliman@bhit.bu.edu.eg

Mostafa Rabah
Professor of Surveying and Geodesy, Department of Civil Engineering, Benha Faculty of Engineering, Benha University, Egypt, mrabah@bhit.bu.edu.eg

Rasha Mohie
Lecturer, Department of Civil Engineering, Benha Faculty of Engineering, Benha University, Egypt, rasha.abdelfattah@bhit.bu.edu.eg

Ahmed Elhadary
Assistant lecturer, Department of Civil Engineering, Benha Faculty of Engineering, Benha University, Egypt, ahmed.elhadari@bhit.bu.edu.eg

Essam Ghanem
Lecturer, Department of Civil Engineering, Benha Faculty of Engineering, Benha University, Egypt, essam.ghanem@bhit.bu.edu.eg

Follow this and additional works at: https://mej.researchcommons.org/home

Assessment of Using UAV Imagery over Featureless Surfaces for Topographic Applications

Ahmed Taha, Mostafa Rabah, Rasha Mohie, Ahmed Elhadary[*] and Essam Ghanim.

Abstract—**The growth and development of Unmanned Aerial Vehicles (UAVs) as a photogrammetric platform, concurrently with the advances in Computer Vision (CV) and image processing algorithms have resulted using UAV Photogrammetry in several topographic applications. CV software algorithms rely on extracting, describing, and matching tie points from the sequences overlapping images to generate 3D colored point clouds. One of the biggest problems obstructing the automated processing of UAV imagery is the featureless of the covered surface. This paper has provided the ability, results, and accuracy of processing images captured by UAVs over non-textured sandy surfaces by providing four aligning and geo-referencing techniques. These four methods, IG/blind matching, IG/reference matching, DG/blind matching, and DG/reference matching, have been presented and tested for 630 aerial images with 80 % overlap and 80 % side lap covered approximately 1 km2 at altitude 178 m above ground level (AGL). The results showed that the captured images could be used to extract the photogrammetric topographical measurements with reliable accuracy. The four techniques' geometric accuracy has ranged between (0.043 m to 0.076 m) & (0.047 m to 0.074) for generated point clouds and linear exterior orientation (EO) parameters, respectively. The indirect geo-referencing with reference matching (IG/reference) recorded the highest-level accuracy of point clouds with 0.043m RMSE compared to the direct geo-referencing with reference matching (DG/reference) which gave the highest geometric accuracy of the linear EO parameters with 0.047m**

I. INTRODUCTION

NOWADAYS, Unmanned Aerial Vehicles (UAVs) are used in a wide range as mobile sensor platforms in many applications such as geography and surveying. The UAVs are equipped with a camera to collect data without any physical contact with the objects. So, the UAV platform can overfly accessible, inaccessible, and dangerous wide areas with high-resolution data in a short time and with little effort, (Mesas-Carrascosa et al., 2016).

Ahmed Taha, Lecturer, Department of Civil Engineering, Benha Faculty of Engineering, Benha University, Egypt (e-mail: ahmed.soliman@bhit.bu.edu.eg).

Mostafa Rabah, Professor of Surveying and Geodesy, Department of Civil Engineering, Benha Faculty of Engineering, Benha University, Egypt (e-mail: mrabah @bhit.bu.edu.eg).

Rasha Mohie, Lecturer, Department of Civil Engineering, Benha Faculty of Engineering, Benha University, Egypt (e-mail: rasha.abdelfattah@bhit.bu.edu.eg).

**Corresponding Author*: Ahmed Elhadary, Assistant lecturer, Department of Civil Engineering, Benha Faculty of Engineering, Benha University, Egypt (e-mail: ahmed.elhadari@bhit.bu.edu.eg)*

Essam Ghanim, Lecturer, Department of Civil Engineering, Benha Faculty of Engineering, Benha University, Egypt (e-mail: essam.ghanem@bhit.bu.edu.eg).

In digital UAV Photogrammetry, image processing by the Structure from Motion (SfM) algorithm is divided into mainly two steps, (Lucieer et al., 2012). The first step is image matching by the Scale-Invariant Feature Transform (SIFT) algorithm, in which raw photos are input. The process automatically extracts key points in the images, describes them, and matches them based on descriptors. So, the surface texture has a significant role and effect in this step. The featureless surface has a complicated process. Fig. 1 shows the differences between the texture and non-textured surfaces, and Fig. 2 shows the workflow of the SfM process.

Image matching can be divided into reference and blind aligning. In the reference aligning method, the overlapping images are only selected based on GNSS linear EO to match. In the blind aligning technique, all the images are chosen to match together by the descriptor tie points (Agisoft, 2019). The second step is the Bundle Adjustment (BA) algorithm, which uses the matching key points that come from image matching and ground control points (GCPs) to determine the interior and exterior orientation parameters for each image and 3D point locations of key points (spare point clouds) (Cramer et al., 2000).

A geo-referencing of the data to the ground coordinate systems is required for topographic applications to determine the objects' spatial locations in a given reference frame. Generally, the geo-referencing can be divided into Direct Georeferencing (DG) using Global Navigational Satellite Systems "GNSS" and Inertial Navigational System "INS" or Indirect Geo-referencing (IG) using GCPs to provide a reference frame for the images (Elsenbeiss et al., 2005). The DG has advantages: faster work, faster processing, simple workflow, and less cost. On the other side, IG has slightly higher accuracy than DG (Rabah et al., 2018).
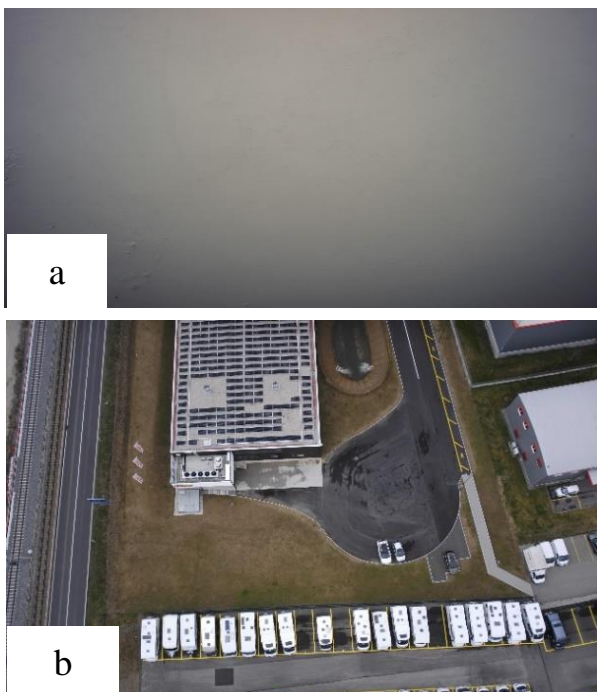

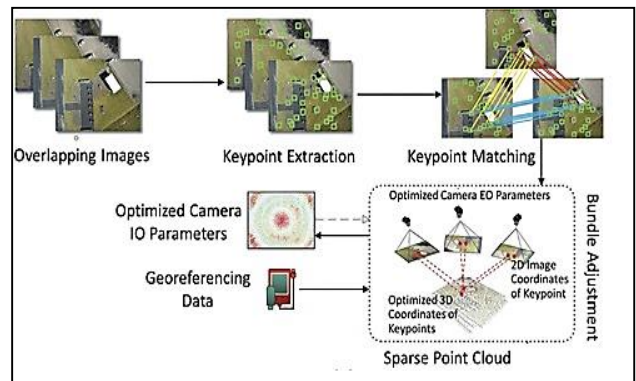Fig. 1: a: images over non-texture flat area, b: images over textured area

Fig. 2: Workflow of SfM processing (Javadnejad, f., et al., 2018).

After applying the SIFT algorithm, the outliers (the wrong matching points) are removed by applying the Random Sample Consensus (RANSAC) algorithm. Fig. 3 shows the differences before and after applying RANSAC (Fonstad et al., 2013).
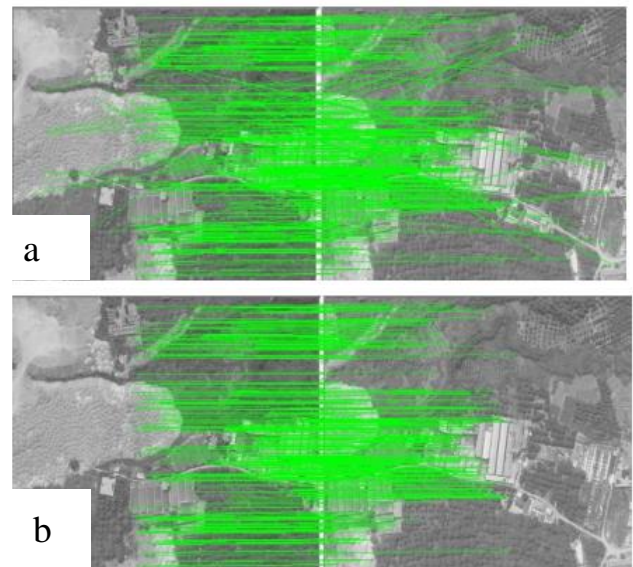

Fig. 3: a: before RANSAC (included wrong matching points), b: after RANSAC (removed wrong matching points)

In image processing, the non-textured of the covered area is one of the most problems obstructing the automated processing of UAV imagery, which prevents the good key points extracting and matching. The current paper investigates the assessment of using UAV imagery over featureless sandy areas by the various types of aligning and geo-referencing. The paper has provided the ability, results, and accuracy of using four techniques of aligning and geo-referencing to process images captured by UAV over featureless sandy areas.

II. RESEARCH METHODOLOGY

A. Area of study:

The experimental site is a 1.03 km X 0.98 km with a general approximate area of 1 km^2 of the non-textured featureless flat sandy area located in Jahra, Kuwait (centered at latitude = 29° 13$^{'}$ 4.54$^{''}$ N, longitude = 47° 39$^{'}$ 45.14$^{''}$ E), Fig. 4 shows the

interest area in Google maps. On July 11, 2019, the photogrammetric test captured 630 images at flying altitude 178 m AGL with a ground sampling distance (GSD) of 4.34 cm/pix and image format 6000x4000 using a 16 mm focal length SONY ILCE-5100 camera.
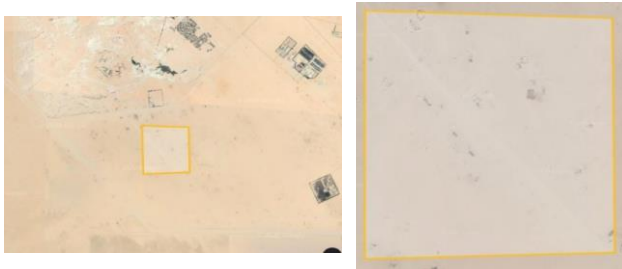

Fig. 4: The test area on Google map.

B. Photogrammetric data acquisition:

Photogrammetric data acquisition has been performed of approximately 178 m AGL using 16 mm focal length SONY ILCE-5100 camera equipped a fixed-wing UAV UX5 vehicle with 1 m Wing length and 2.5 kg weight. Fig. 5 shows the UAV shape and the used camera, and the UAV characteristics are shown in table 1.

Fig. 5: The UX5 UAV and the used SONY camera

630 aerial images were captured with 80% for both overlap and side lap, which are high enough to process and align these non-textured images in the photogrammetric algorithms. Fig. 6 shows samples of the images. 12 ground control and checkpoints are determined by GNSS static post-processing and distributed over all the area. Besides, the linear exterior orientation (EO) parameters (the camera location position) for each image were calculated using RTK-GNSS in the world geodetic system 1984 "WGS84".

TABLE 1
THE CHARACTERISTICS OF THE UAV (TRIMBLE, 2021).

Endurance	Up to 50 min
Weight	2.5 kg
Wingspan	1 m
Material	EPP foam; carbon frame structure; composite elements
Cruise speed	80 km/h
Flying range	60 km
Sensor (Camera)	Sony ilce-5100
Resolution	24 Mpix
Image format	6000 * 4000

Fig. 6: Sample of the UAV aerial images.

C. Photogrammetric data processing:

The photogrammetric flight produced 630 images which were processed with Agisoft Metashape software in the reference system WGS84. Twelve ground points were used for geo-referencing and checkpoints. Agisoft Metashape software is one of the most simple, cheap, and accurate image processing (Gross and Heumann, 2016). Firstly, the key points are detected in the overlapping images, then described by SIFT algorithms. Finally, the descriptor points are matched, and object reconstruction is created. The wrong matching points in the matching process are removed by RANSAC (Agisoft, 2019). The geo-referencing is applied for generating the 3D point cloud and model in the reference coordinate system. The Agisoft parameters processing are shown in table 2, and the flowchart of field data collection and image processing steps are shown in Fig. 7

TABLE 2
THE FIELD DATA COLLECTION, CAMERAM AND AGISOFT
PARAMETERS PROCESSING.

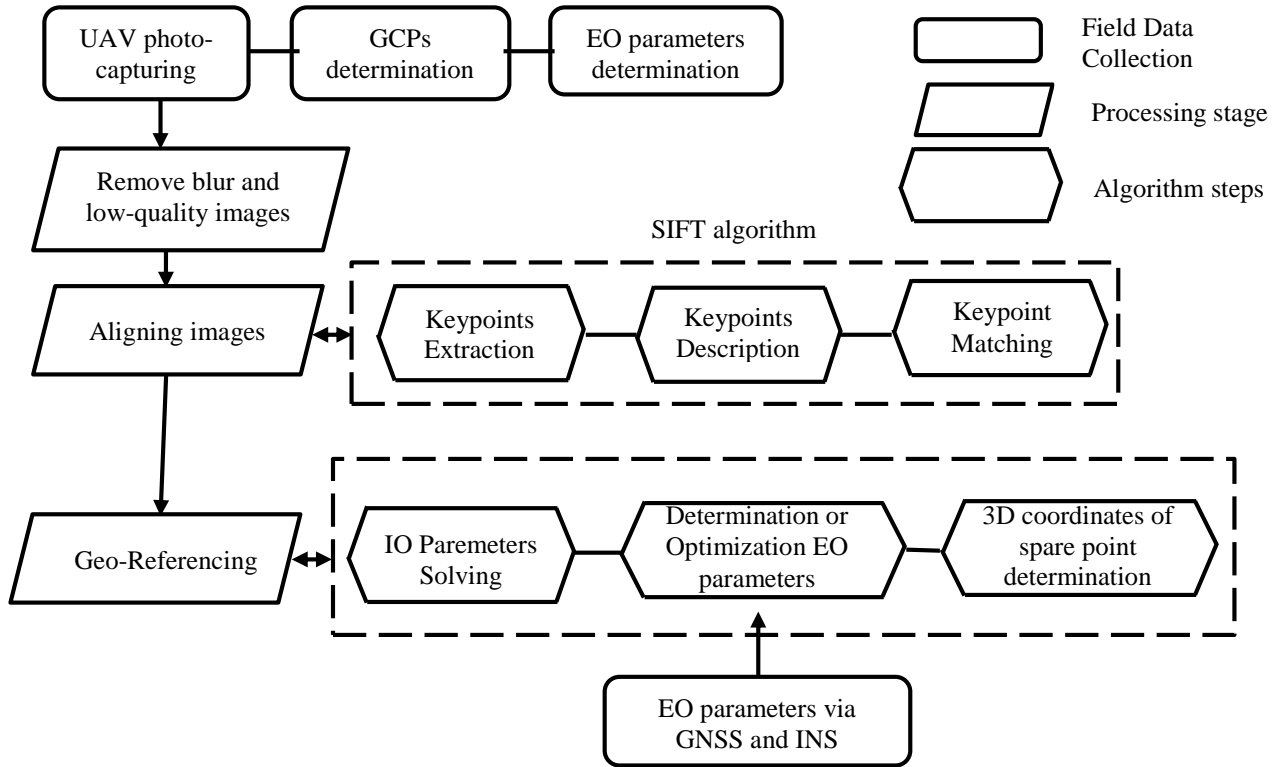| No. of images	630
Flying altitude	178 m
Ground sampling distance (GSD)	4.34 cm/pix
Coverage area	1 km2 (1.03 km x 0.98 km)
Image format	6000 x 4000
Camera	SONY ILCE-5100
Focal length	16 mm
Key point per image	10000
Tie point per image	1000

Fig. 7: Flowchart of field data collection and image processing stages

III.   RESULTS AND DISCUSSIONS:

Twelve ground points have been determined by static GNSS with 0.009 m spatial accuracy. For the IG process, five points distributed uniformly over all the area were used as GCPs. The other seven ground points were used as independent checkpoints (ICPs) to check the geometric accuracy. The layout of the GCPs and ICPs locations and the planning of the flight are shown in Fig. 8. Fig. 9 shows the identification of the GCPs in the images. For the DG process, the linear EO parameters derived by RTK-GNSS, with 0.02 m spatial accuracy, were used for geo-referencing without needing any GCPs.
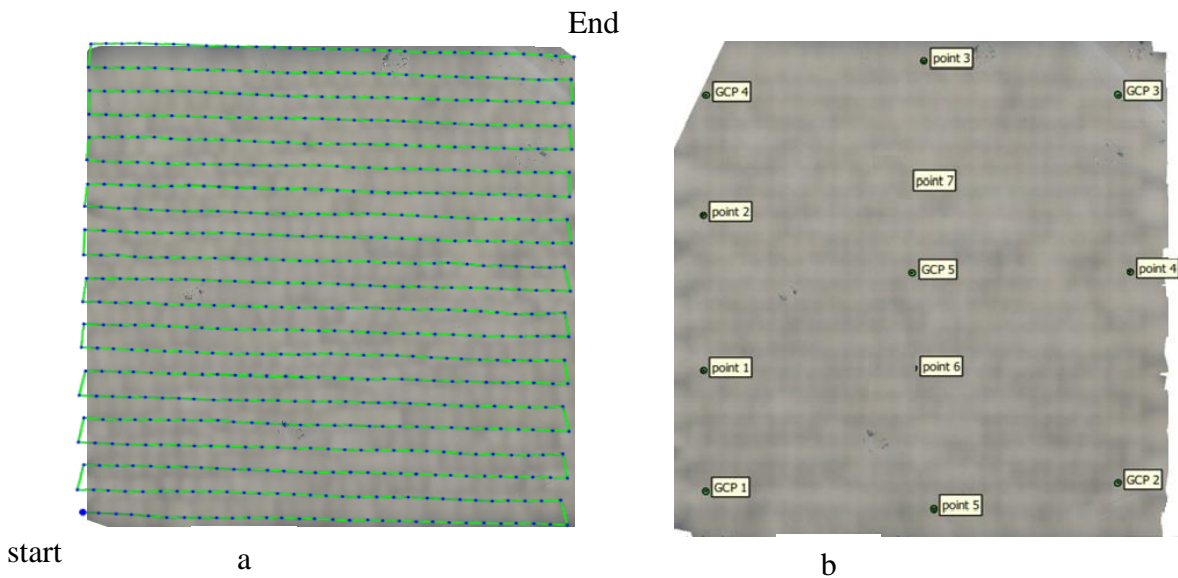

Fig. 8: a: The flight planning, The green line follows the position of the images starting from the large blue dot. b: The locations of 5 GCPs (Orange Triangle) and 7 ICPs (Red Cross).
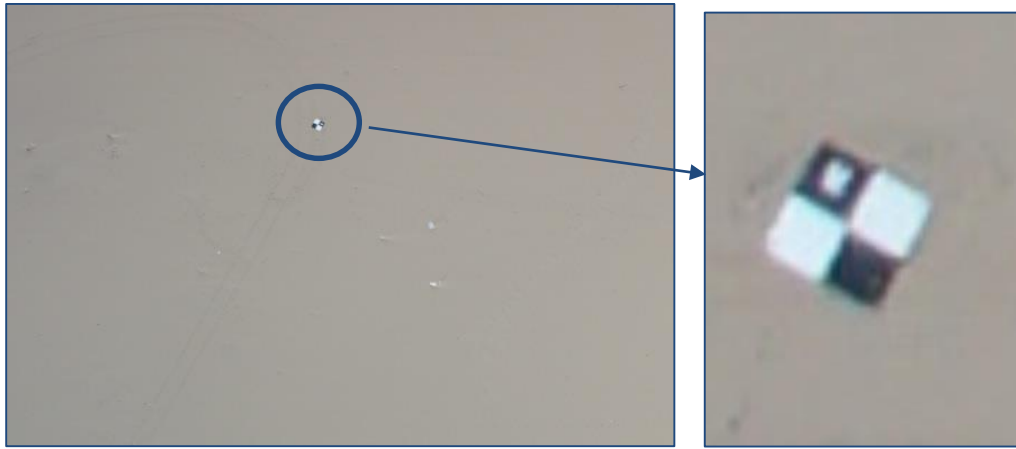
Fig. 9: Identification of GCPs in images

For geometric accuracy, RMSE was calculated for ICPs as a difference between the static GNSS as reference data and UAV data (FGDC, 1998).

$$RMSE_X = \sqrt{\frac{\Sigma(X_{GNSS}-X_{UAV})^2}{n}}$$

$$RMSE_Y = \sqrt{\frac{\Sigma(Y_{GNSS}-Y_{UAV})^2}{n}}$$

$$RMSE_{XY} = \sqrt{RMSE_X{}^2 + RMSE_Y{}^2}$$

$$RMSE_Z = \sqrt{\frac{\Sigma(Z_{GNSS}-Z_{UAV})^2}{n}}$$

$$RMSE_{XYZ} = \sqrt{RMSE_X{}^2 + RMSE_Y{}^2 + RMSE_Z{}^2}$$

As it is illustrated in Fig. 10, image processing consists of two stages, image matching and geo-referencing. The first stage, image aligning, is divided into two techniques blind and reference. In the reference aligning method, the overlapping images are only selected based on GNSS linear EO to be matched. In the blind aligning technique, all the images are chosen to be matched together by the descriptor tie points. The second stage is the geo-referencing divided into direct and indirect, where the Bundle Adjustment (BA) is applied for both.
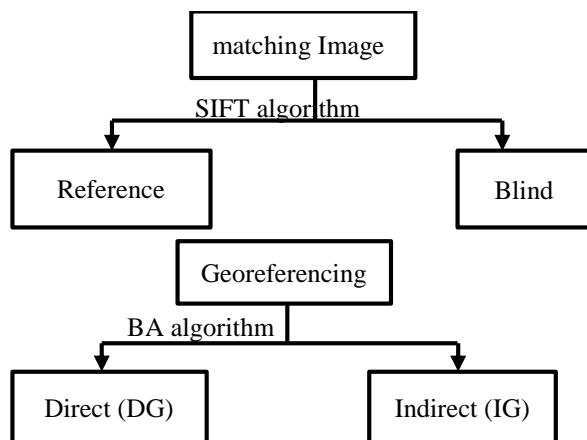

Fig. 10: Image matching and geo-referencing types

In this study, four techniques of aligning and geo-referencing have been presented and studied to assess the ability and accuracy of using aerial images captured by UAV over featureless sandy areas. The four techniques were (1) IG/blind aligning, (2) IG/reference aligning, (3) DG/blind aligning, and (4) DG/reference aligning.

A. The assessment of IG/blind technique:

In this section, the Geometric accuracy of UAV point clouds obtained by the IG/blind method was presented by statistical analysis of the differences obtained by comparing ICPs derived from the IG/blind method and static GNSS as a reference. Results are summarized in Table 3 and plotted in Fig. 11. In addition to the linear EO parameters accuracy, the differences in camera position determined by an on-board RTK-GNSS as a reference and positioning resulting from the IG/blind process are computed and plotted in table 4 and Fig. 12.

TABLE 3
ERRORS AND RMSE OF ICPS FOR IG/BLIND TECHNIQUE.

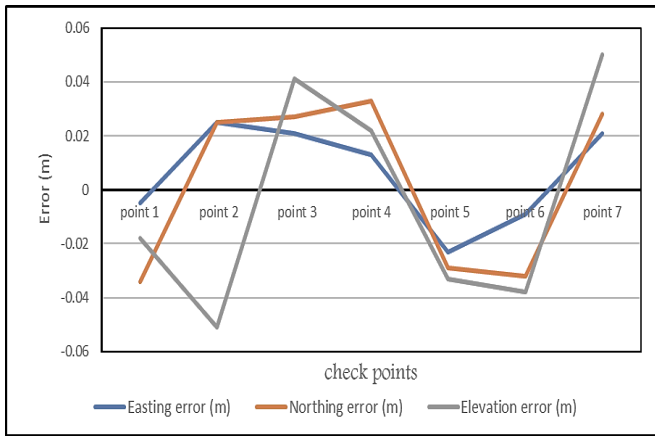| Point No.	Easting error (m)	Northing error (m)	Elevation error (m)	Total error (m)
Point 1	-0.005	-0.034	-0.018	0.039
Point 2	0.025	0.025	-0.051	0.062
Point 3	0.021	0.027	0.041	0.053
Point 4	0.013	0.033	0.022	0.042
Point 5	-0.023	-0.029	-0.033	0.05
Point 6	-0.009	-0.032	-0.038	0.05
Point 7	0.021	0.028	0.050	0.061
Total RMSE	0.018	0.030	0.038	0.052

Fig. 11: ICPs Errors for IG/blind aligning technique

As it is shown in table 3 and Fig. 11, The processing by the IG/blind resulted to 0.052 m accuracy of the produced point clouds with minimum of the absolute values of errors of 0.039 m and a maximum of the absolute value of 0.062 m. The RMSE of easting, northing, and elevation were 0.018 m, 0.03 m, and 0.038m, respectively. The maximum and the minimum of the absolute values of errors of easting are 0.025 & 0.005 m, northing are 0.034 & 0.025 m, and elevation were 0.051 & 0.018 m, respectively.

From table 4 and Fig. 12, one can easily find that about 90% of the errors in linear EO parameters derived by the IG/blind method was within (-0.06 m to 0.05 m), (-0.048 m to 0.040 m), and (-0.08 m to -0.048 m) for easting, northing, and elevation, respectively. The mean of the absolute values of errors and RMSE for easting are 0.023 & 0.036 m, northing were 0.021 & 0.026 m and elevation were 0.062 & 0.063 m respectively. The maximum and the minimum of the absolute values of errors in easting are 0.10 & 0.001 m, northing are 0.072 & 0 m, and elevation were 0.096 & 0.041 m, respectively. The above results demonstrated that the IG/blind matching method is appropriate for processing UAV images over featureless surfaces and achieving centimeters accuracy.
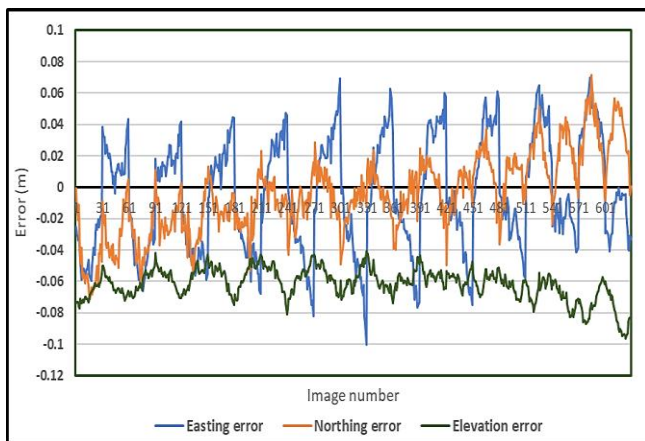

Fig. 12: The differences between linear EO derived by IG/blind aligning technique and RTK-GNSS.

TABLE 4
ERRORS OF LINEAR EO PARAMETERS FOR IG/BLIND TECHNIQUE

	Easting Error (m)	Northing Error (m)	Elevation Error (m)
Mean (m)	0.023	0.021	0.062
RMSE (m)	0.026	0.023	0.065
Max. Error (m)	-0.100	0.072	-0.096
Min. Error (m)	-0.001	0	-0.041
90 % of errors locates between	-0.06 to 0.05	-0.048 to 0.040	-0.08 to -0.048

B. The accuracy of DG/blind technique:

The geo-referencing is performed using the computed three linear EO parameters by RTK-GNSS rather than GCPs. The same seven ICPs used in the IG are used in the DG to determine the geometric accuracy of the generated UAV point clouds. The geometric accuracy of generated point clouds is shown in table 5 and Fig. 13. The statistical values of the linear EO parameters errors are listed and reported in table 6 and Fig. 14.

TABLE 5
ERRORS AND RMSE OF ICPS FOR DG/BLIND TECHNIQUE

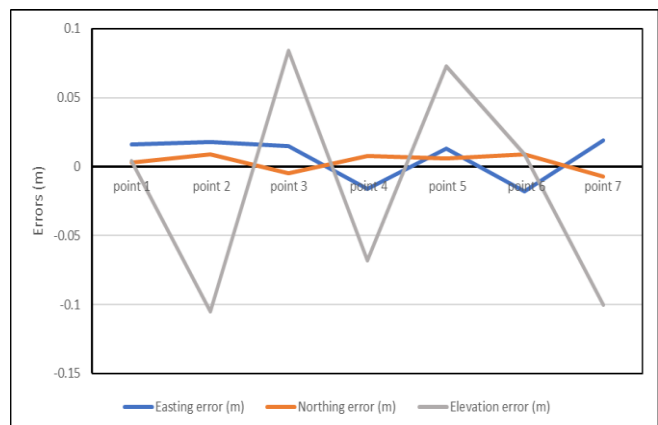|	Easting error (m)	Northing error (m)	Elevation error (m)	Total error (m)
Point 1	0.016	0.003	0.004	0.017
Point 2	0.018	0.009	-0.105	0.107
Point 3	0.015	-0.005	0.084	0.085
Point 4	-0.016	0.008	-0.068	0.07
Point 5	0.013	0.006	0.073	0.074
Point 6	-0.018	0.009	0.009	0.022
Point 7	0.019	-0.007	-0.1	0.102
Total RMSE	0.017	0.007	0.074	0.076

Fig. 13: ICPs Errors for DG/blind aligning technique

Based on table 5 and Fig. 13, it can conclude that RMSE was 0.076 m, while each individual RMSE for Easting, Northing and elevation recorded 0.017 m, 0.07 m and 0.074 m, respectively. RMSE analysis was based on the seven checkpoints that were established evenly at the study area. The maximum and the minimum of the absolute values of errors of easting, northing, and elevation were (0.019 & 0.013 m), (0.009 & 0.003 m), (0.105 & 0.004 m), respectively. Both easting and northing have small errors compared to elevation which have the high error affecting on the total RMSE.
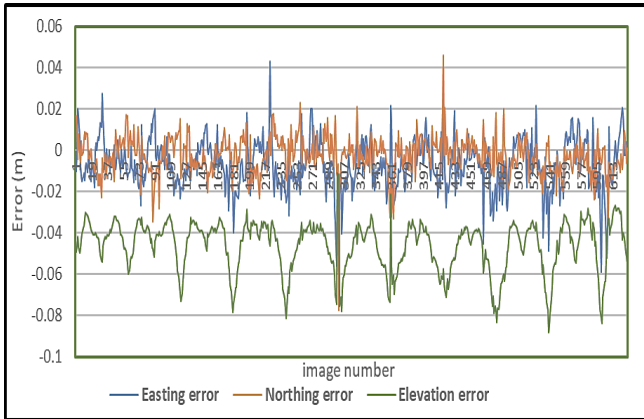

Fig. 14: The differences between linear EO derived by DG/blind aligning technique and RTK-GNSS

TABLE 6
ERRORS OF LINEAR EO PARAMETERS FOR DG/BLIND TECHNIQUE

	Easting Error (m)	Northing Error (m)	Elevation Error (m)
Absolute Mean (m)	0.011	0.007	0.046
RMSE (m)	0.014	0.01	0.048
Max. Error (m)	-0.06	-0.078	-0.088
Min. Error (m)	0	0	0.001
90 % of errors locates between	-0.026 to 0.013	-0.016 to 0.01	-0.071 to -0.033

Table 6 and Fig. 14 show that the mean of the absolute values of errors of the linear EO parameters for the easting, northing, and elevation recorded 0.011 m, 0.007 m, and 0.046 m, respectively. In comparison, the RMSE recorded 0.014 m, 0.01 m, and 0.48 m for easting, northing, and elevation, respectively. The maximum of the absolute values of errors of linear EO parameters was 0.06m, 0.078m, and 0.088m for easting, northing, and elevation, respectively, while the minimum for both easting and northing was around zero and 0.001 m for elevation. About 90% of the linear EO parameters errors located between (-0.026 to 0.013) m, (-0.016 to 0.01) m, and (-0.071 to -0.033) m in easting, northing, and elevation, respectively. In general, the DG/blind process is capable of processing featureless UAV images with centimeters accuracy.

C. The accuracy of IG/reference technique:

The image processing via IG/reference method was assessed using the ICPs to report the accuracy of the generated point clouds against the true ground point obtained from the static GNSS system. The results are listed and plotted in Table 7, and Fig. 15. In addition to the linear EO parameters accuracy, different statistical between on-board RTK-GNSS and positioning resulting from IG/reference process, were applied and plotted in table 8 and figure 16.

TABLE 7
ERRORS AND RMSE OF ICPS FOR IG/REFERENCE TECHNIQUE

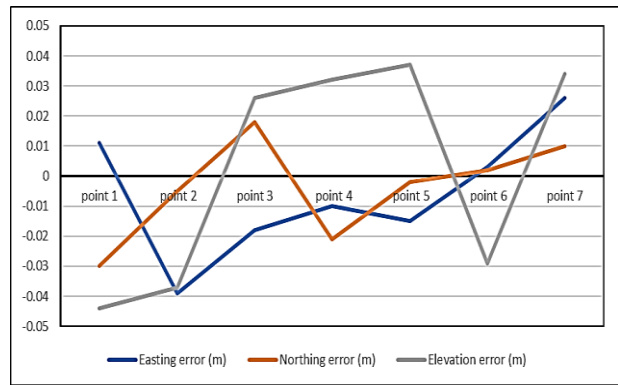|	Easting error (m)	Northing error (m)	Elevation error (m)	Total error (m)
point 1	0.011	-0.03	-0.044	0.054
point 2	-0.039	-0.005	-0.037	0.054
point 3	-0.018	0.018	0.026	0.036
point 4	-0.01	-0.021	0.032	0.04
point 5	-0.015	-0.002	0.037	0.04
point 6	0.003	0.002	-0.029	0.029
point 7	0.026	0.01	0.034	0.044
Total RMSE	0.020	0.016	0.035	0.043

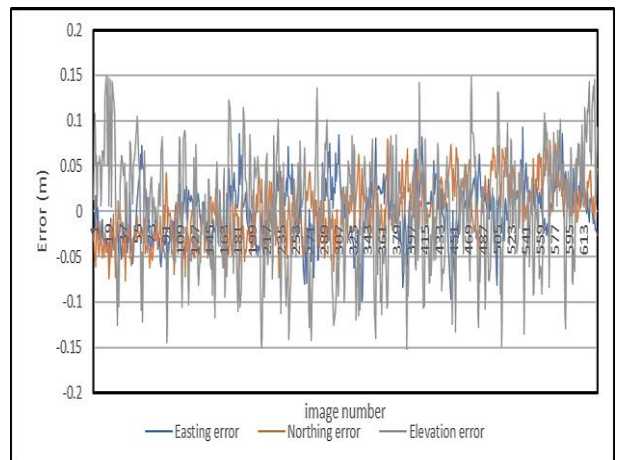Fig. 15: ICPs Errors for IG/reference aligning technique

Fig. 16: The differences between linear EO derived by IG/reference aligning technique and RTK-GNSS.

TABLE 8
ERRORS OF LINEAR EO PARAMETERS FOR IG/REFERENCE
TECHNIQUE

	Easting Error (m)	Northing Error (m)	Elevation Error (m)
Absolute Mean (m)	0.025	0.026	0.051
RMSE (m)	0.027	0.029	0.056
Max. Error (m)	-0.099	0.079	-0.15
Min. Error (m)	0	0	0.002
90 % of errors locates between	-0.0526 to 0.049	-0.05 to 0.055	-0.106 to 0.099

Table 7 and Fig. 15 show the errors of UAV point clouds derived by the IG/reference method. The height had the highest RMSE, while the northing had the lowest. The peak error, RMSE, and the minimum of the absolute values of errors in easting recorded (0.039, 0.020 & 0.003 m), northing recorded (0.03, 0.016 & 0.002 m) and height recorded (0.044, 0.035 & 0.026 m), respectively.

As it is illustrated in table 8 and Fig. 16, The peak, RMSE, the mean of the absolute values of errors, and the minimum of the absolute values of errors of linear EO parameters for easting, northing, and elevation were (0.099, 0.027, 0.025, 0 m), (0.079, 0.029, 0.026, 0 m), and (0.15, 0.056, 0.051, 0.002 m), respectively. About 90% of the linear EO parameters errors of easting was confined between (-0.0526 to 0.049) m, northing was confined between (-0.05 to 0.055) m, and elevation was located between (-0.106 to 0.99) m.

Generally, The DG/reference process gave a geometric accuracy of 0.043 m of the generated point cloud. This result reveals that the DG/reference is appropriate for processing UAV images over featureless surfaces, achieving centimeters accuracy in all axis.

D. The accuracy of dg/reference technique:

The three linear EO parameters are computed by RTK-GNSS. The spatial accuracy of the obtained UAV point clouds is shown in table 9 and Fig. 17. The computed linear EO parameters evaluation is computed and plotted in table 10 and Fig. 18.

TABLE 9
ERRORS AND RMSE OF ICPS FOR DG/REFERENCE TECHNIQUE

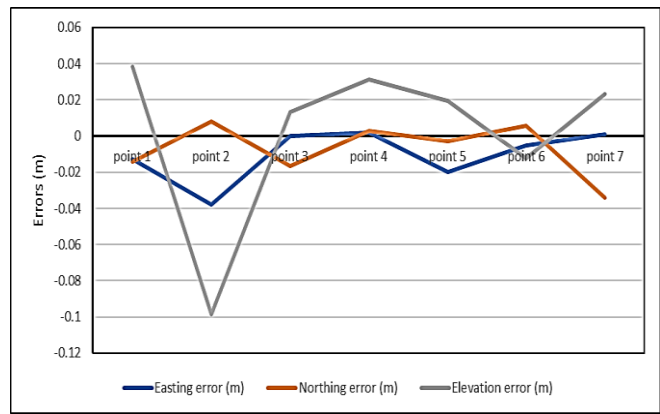|	Easting error (m)	Northing error (m)	Elevation error (m)	Total error (m)
point 1	-0.013	-0.014	0.038	0.0429
point 2	-0.038	0.008	-0.099	0.106
point 3	0.001	-0.017	0.013	0.021
point 4	0.002	0.003	0.031	0.032
point 5	-0.020	-0.003	0.019	0.028
point 6	-0.005	0.006	-0.012	0.014
point 7	0.001	-0.034	0.023	0.042
Total RMSE	0.017	0.016	0.044	0.050

Fig. 17: ICPs Errors for DG/reference aligning technique

TABLE 10
ERRORS OF LINEAR EO PARAMETERS FOR DG WITH REFERENCE
ALIGNING TECHNIQUE

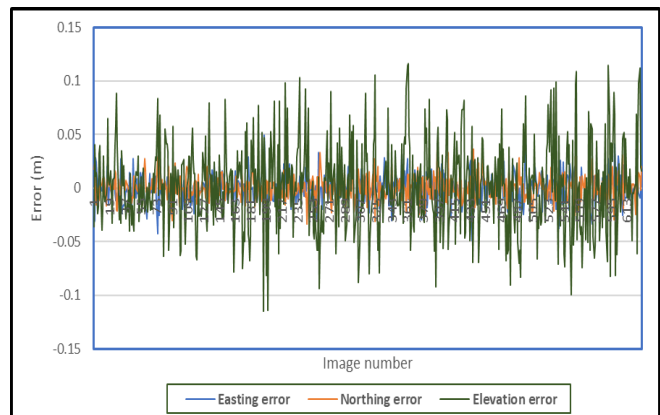|	Easting Error (m)	Northing Error (m)	Elevation Error (m)
Absolute Mean (m)	0.012	0.01	0.039
RMSE (m)	0.016	0.014	0.042
Max. Error (m)	0.05	0.04	0.116
Min. Error (m)	0	0	0
90 % of errors locates between	-0.022 to 0.026	-0.019 to 0.021	-0.078 to 0.084

Fig. 18: The differences between linear EO derived by DG/reference and RTK-GNSS

As shown in table 9 and Fig. 17, it is easy to conclude that the RMSE of UAV point derived by DG/reference reached 0.05m. The elevation has the highest RMSE. Northing and easting had approximately the same RMSE. The maximum and the minimum of the absolute values of errors of easting were 0.038 & 0.001m, northing were 0.034 & 0.003m and elevation were 0.099 & 0.012m.

Table 10 and Fig. 18 show that the mean of the absolute values of errors and RMSE of linear EO parameters for easting equaled 0.012 & 0.016 m, northing equaled 0.01 & 0.014 m and elevation equaled 0.039 & 0.042 m respectively. About 90% of the errors in easting, northing, and elevation located between (-0.022 to 0.026) m, (-0.019 to 0.021) m, and (-0.078 to 0.084) m, respectively. The maximum of the absolute values of errors

in easting, northing, and elevation were 0.05 m, 0.04 m, and 0.116 m, respectively. The minimum of the absolute values of errors for the three axes is approximately equal to zero m. On the whole, The DG/reference aligning can process UAV images over flat areas in centimeters accuracy for both UAV point clouds and linear EO parameters.

E. The assessment and comparison of the performed four techniques:

To assess the accuracy and robustness of the produced UAV 3D models, tables 11 & 12 and figures 19 & 20 summarize the produced point cloud and linear EO parameters accuracies according to the ICPs for the four processing techniques.

TABLE 11
ACCURACY OF THE DERIVED UAV POINT CLOUDS OF THE FOUR TECHNIQUES.

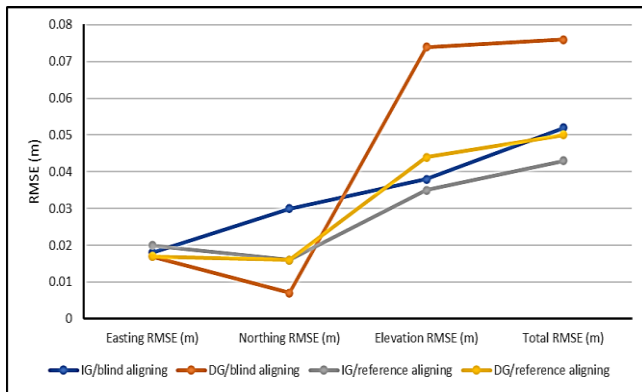|	Easting RMSE (m)	Northing RMSE (m)	Elevation RMSE (m)	Total RMSE (m)
IG/blind aligning	0.018	0.03	0.038	0.052
DG/blind aligning	0.017	0.007	0.074	0.076
IG/reference aligning	0.02	0.016	0.035	0.043
DG/reference aligning	0.017	0.016	0.044	0.050

Fig. 19: Comparison of the derived UAV point clouds accuracy of the four techniques.

Table 12
Accuracy of the linear EO parameters of the four techniques.

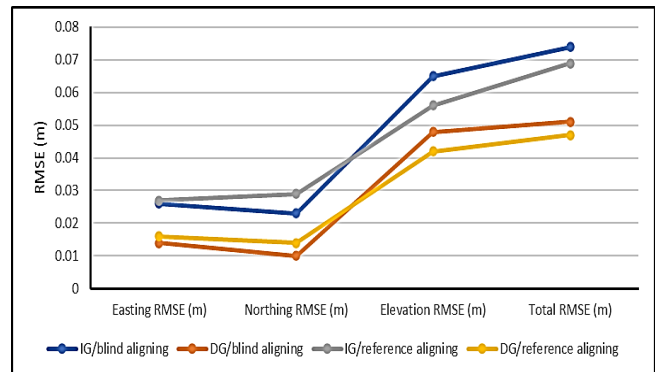|	Easting RMSE (m)	Northing RMSE (m)	Elevation RMSE (m)	Total RMSE (m)
IG/blind aligning	0.026	0.023	0.065	0.074
DG/blind aligning	0.014	0.01	0.048	0.051
IG/reference aligning	0.027	0.029	0.056	0.069
DG/reference aligning	0.016	0.014	0.042	0.047

Fig. 20: Comparison of the EO parameters accuracy of the four techniques.

Based on tables 11 & 12 and figures 19 & 20, The accuracy of the four techniques has shown that UAV images are a useful tool for producing accurate topographic measurements over featureless surfaces. However, the accuracies of the produced point clouds are close to 0.050 m for all the different techniques except DG/blind method records accuracy around 0.076 m. In the four cases, larger accuracy is present along the IG/reference method with an overall accuracy of 0.043 m. The results of the linear EO parameters accuracy reveal notable differences for the four different techniques. The accurate results are recorded by DG/reference method compared to IG/blind records the worse accuracy by 0.074 m.

On the whole, the four techniques recorded geometric accuracy between (0.043 to 0.076) m for generated point clouds and (0.047 to 0.074) m for linear EO parameters. Thus, UAV imagery over a non-textured area is an appropriate technique for generating 3D colored point clouds, orthomosaic, DSM, contour maps, and other topographic output products in centimeters accuracy.

IV. CONCLUSION

The focus of this study was to assess the ability, results, and accuracy of using UAV images over featureless sandy areas in topographic measurements. Four methods have been presented and tested for 630 aerial photographs covered 1 km^2 at altitude 178 m AGL.

The images captured by UAVs over featureless sandy areas can be used to extract the topographic measurements with centimeters accuracy. The accuracy of the four techniques of the produced point clouds is close to 0.050 m for both IG/reference, DG/reference, and IG/blind methods compared to DG/blind method records accuracy around 0.076 m. larger accuracy is present along the IG/reference method with an overall accuracy of 0.043 m. The accurate results of the linear EO parameters are recorded by DG/reference method compared to IG/blind records the worse accuracy by 0.074 m. On the whole, the four techniques record geometric accuracy between (0.043 to 0.076) m for generated point clouds and (0.047 to 0.074) m for linear EO parameters.

AUTHORS CONTRIBUTION:

Ahmed Taha did the following:
(Project administration, Supervision, Final approval of the version to be published)

Mostafa.Rabah did the following:
(Conception or design of the work, Data collection and tools, Data analysis and interpretation, Project administration, Supervision, Final approval of the version to be published)

Rasha Mohie did the following:
(Supervision, Final approval of the version to be published)

Ahmed Elhadary did the following:
(Design of the work, Data collection and tools, Data analysis and interpretation, Funding acquisition, Resources, Methodology, Drafting the article, Critical revision of the article, Final approval of the version to be published)

Essam Ghanem did the following:
(Supervision, Final approval of the version to be published)

▪ All authors have participated in
a. conception and design, or analysis and interpretation of the data
b. drafting the article or revising it critically for important intellectual content
c. approval of the final version.

REFERENCES:
[1] Agisoft, 2019. Agisoft Metashape User Manual: Professional Edition, Version1.6. < https://www.agisoft.com/pdf/metashape-pro_1_6_en.pdf>.
[2] Cramer, M., Stallmann, D. and Haala, N., 2000. Direct Geo-Referencing Using GPS/Inertial Exterior Orientations for Photogrammetric Applications. Remote Sensing. Vol. 33, Part B3, pp. 198-205.
[3] Eisenbeiss, H., and Zhang, L., 2006. Comparison of DSMs Generated from Mini UAV Imagery and Terrestrial Laser Scanner in a Cultural Heritage Application. ISPRS Commission V Symposium' Image Engineering and Vision Metrology. XXXVI (5), 90-96.
[4] FGDC, 1998. Geospatial Positioning Accuracy Standards. FGDC-STD-007.3-1998, Part 3: National Standard for Spatial Data Accuracy (NSSDA).
[5] Fonstad, M., Dietrich, J., Courville, B., Jensen, J. and Carbonneau, P., 2013. Topographic structure from motion: a new development in photogrammetric measurement. Earth Surface Processes and Landforms. Vol. 38, pp. 421-430.
[6] Gross, J.W., Heumann, B.W., 2016. A statistical examination of image stitching software packages for use with unmanned aerial systems. Photogramm. Eng. Remote Sens. 82 (6), 419–425.
[7] Javadnejad, f., Gillins, D., Parrish, C. and Slocum, R., 2019. A photogrammetric approach generation to fusing natural colour and thermal infrared UAS imagery in 3D point cloud. International journal of remote sensing. 41(1), 211-237.
[8] Lucieer, A., Robinson, S., Turner, D., Harwin, S., and Kelcey, J., 2012. Using a micro-UAV for ultra-high resolution multi-sensor observations of Antarctic moss beds. Remote Sensing and Spatial Information Sciences. XXXIX(B1), 429-433.
[9] Mesas-Carrascosa, F. J., Notario García, M. D., Meroño de Larriva, J. E., and García-Ferrer, A., 2016. An Analysis of the Influence of Flight Parameters in the Generation of Unmanned Aerial Vehicle (UAV) Orthomosaicks to Survey Archaeological Areas. Sensors (Basel, Switzerland). 16 (11), 18-38.
[10] Rabah, M., Basiouny, M., Ghanem, E. and Elhadary, A., 2018. Using RTK and VRS in direct geo-referencing of the UAV imagery. NRIAG Journal of Astronomy and Geophysics. 7 (2), 220-226.
[11] Trimble, 2021. Trimble UX5 Unmanned Aircraft System. http://www.kmcgeo.com/Datasheets/UX5.pdf.

TITLE ARABIC:

تقييم استخدام صور الطائرات بدون طيار للتطبيقات الطبوغرافية
فوق الأسطح المستوية

ABSTRACT ARABIC:

أدي التطور في الطائرات بدون طيار كمنصات للتصوير الجوي بالتزامن مع التقدم في الرؤية الحاسوبية computer vision وخوارزميات معالجة وتحليل الصور إلى التوسع في التصوير الجوي باستخدام الطائرات بدون طيار في العديد من التطبيقات الطبوغرافية. تعد الاسطح المستوية الخالية من المعالم featureless واحدة من أكبر المشاكل التي تعيق المعالجة الآلية للصور الجوية، يقدم هذا البحث دراسة قدرة ونتائج ودقة معالجة الصور الملتقطة باستخدام الطائرات بدون طيار فوق الاسطح المستوية من خلال دراسة أربع تقنيات من المعالجة، تم اختبار هذه الطرق باستخدام 630 صورة جوية مع تداخل امامي وجانبي 80% تغطي حوالي 1 كيلومتر مربع تقريبا على ارتفاع 178 متر فوق سطح الأرض. أظهرت النتائج انه يمكن استخدام الصور الملتقطة لاستخراج القياسات الطبوغرافية بدقة تراوحت بين (0.043 إلى 0.076 متر) و (0.047 إلى 0.074 متر) للسحابة النقطية المنتجة وعناصر التوجيه الخطي الخارجي على التوالي. سجلت طريقة IG/reference اعلي دقة للسحابة النقطية مقارنة بـ DG/reference التي سجلت اعلي دقة لتحديد عناصر التوجيه الخارجي.